Quantitative modeling of tumor dynamics and development of drug resistance in non-small cell lung cancer patients treated with erlotinib

Anyue Yin[1] | G. D. Marijn Veerman[2] | Johan G. C. van Hasselt[3] | Christi M. J. Steendam[4,5] | Hendrikus Jan Dubbink[6] | Henk-Jan Guchelaar[1] | Lena E. Friberg[7] | Anne-Marie C. Dingemans[4] | Ron H. J. Mathijssen[2] | Dirk Jan A. R. Moes[1]

[1]Department of Clinical Pharmacy and Toxicology, Leiden University Medical Center, Leiden, The Netherlands

[2]Department of Medical Oncology, Erasmus MC Cancer Institute, Rotterdam, The Netherlands

[3]Division of Systems Pharmacology and Pharmacy, Leiden Academic Centre for Drug Research (LACDR), Leiden University, Leiden, The Netherlands

[4]Department of Pulmonary Diseases, Erasmus MC Cancer Institute, Rotterdam, The Netherlands

[5]Department of Pulmonary Diseases, Catharina Hospital, Eindhoven, The Netherlands

[6]Department of Pathology, Erasmus MC Cancer Institute, Rotterdam, The Netherlands

[7]Department of Pharmacy, Uppsala University, Uppsala, Sweden

Correspondence
Dirk Jan A. R. Moes, Albinusdreef 2, 2333 ZA Leiden, The Netherlands.
Email: d.j.a.r.moes@lumc.nl

Funding information
Roche

Abstract

Insight into the development of treatment resistance can support the optimization of anticancer treatments. This study aims to characterize the tumor dynamics and development of drug resistance in patients with non-small cell lung cancer treated with erlotinib, and investigate the relationship between baseline circulating tumor DNA (ctDNA) data and tumor dynamics. Data obtained for the analysis included (1) intensively sampled erlotinib concentrations from 29 patients from two previous pharmacokinetic (PK) studies, and (2) tumor sizes, ctDNA measurements, and sparsely sampled erlotinib concentrations from 18 patients from the START-TKI study. A two-compartment population PK model was first developed which well-described the PK data. The PK model was subsequently applied to investigate the exposure-tumor dynamics relationship. To characterize the tumor dynamics, models accounting for intra-tumor heterogeneity and acquired resistance with or without primary resistance were investigated. Eventually, the model assumed acquired resistance only resulted in an adequate fit. Additionally, models with or without exposure-dependent treatment effect were explored, and no significant exposure-response relationship for erlotinib was identified within the observed exposure range. Subsequently, the correlation of baseline ctDNA data on *EGFR* and *TP53* variants with tumor dynamics' parameters was explored. The analysis indicated that higher baseline plasma *EGFR* mutation levels correlated with increased tumor growth rates, and the inclusion of ctDNA measurements improved model fit. This result suggests that quantitative ctDNA measurements at baseline have the

Anyue Yin and G. D. Marijn Veerman should be considered joint first authors.

potential to be a predictor of anticancer treatment response. The developed model can potentially be applied to design optimal treatment regimens that better overcome resistance.

Study Highlights

WHAT IS THE CURRENT KNOWLEDGE ON THE TOPIC?

Insight into the evolutionary development of treatment resistance can support the optimization of anticancer treatments. This is also the case in patients with non-small cell lung cancer (NSCLC). A model-based approach can support such study based on data on pharmacokinetics, tumor sizes, and genetic biomarkers.

WHAT QUESTION DID THIS STUDY ADDRESS?

We aimed to quantitatively characterize the tumor dynamics and evolving resistance development in patients with NSCLC treated with erlotinib, and investigate the relationship between baseline circulating tumor DNA (ctDNA) measurements and tumor dynamics.

WHAT DOES THIS STUDY ADD TO OUR KNOWLEDGE?

A model accounting for intra-tumor heterogeneity and acquired resistance well-characterized the tumor size dynamics in patients with NSCLC during erlotinib treatment. No exposure-tumor inhibition relationship was identified in the identified exposure range. Baseline ctDNA data on mutant *EGFR* levels correlate with tumor growth rate and the inclusion of ctDNA data improved model prediction.

HOW MIGHT THIS CHANGE DRUG DISCOVERY, DEVELOPMENT, AND/OR THERAPEUTICS?

Our findings suggest that baseline ctDNA measurements have the potential to be a predictor of anticancer treatment response, which encouraged to use ctDNA as an early biomarker. The developed model can further be applied to design optimal treatment regimens to better overcome resistance.

INTRODUCTION

The occurrence of anticancer treatment resistance due to intra-tumor heterogeneity and evolving adaptation of tumor cells to the treatment can limit the long-lasting efficacy of targeted anticancer treatment.[1,2] In order to improve the anticancer treatment outcome, it is important to have detailed insight into the tumor progression during treatment because it enables designing of alternative treatment strategies.

In patients with non-small cell lung cancer (NSCLC), erlotinib, a tyrosine kinase inhibitor (TKI), is one of the effective treatment options especially for patients with *EGFR* exon 19 deletions or exon 21 mutations.[3–5] However, the occurrence of acquired drug resistance, which is most frequently due to the acquisition of the *EGFR* p.T790M mutation, and the possible presence of drug-resistant component pretreatment (primary resistance) can limit its efficacy and result in relapse.[3–6]

Thus, understanding the evolving progression of NSCLC during the treatment and identifying predictive biomarkers would be beneficial to optimize the treatment of NSCLC.

Pharmacometric modeling allows quantitative characterization and prediction of pharmacokinetic (PK) – pharmacodynamic (PD) profiles of drugs and thus facilitates treatment design.[7–9] With the help of a model-based approach, studies on evolving tumor progression can be conducted based on available data on tumor sizes and genetic biomarkers, and optimal treatment designs can be evaluated. Our previous study has proven such a concept based on data from patients with metastatic colorectal cancer as well as from patients with NSCLC.[10] Further incorporating the exposure of therapeutic agents in the model can support the investigation and understanding of exposure-tumor inhibition relationship and the evolutionary tumor dynamics in relation to drug exposure during anticancer treatment.

Circulating tumor DNA (ctDNA), which are DNA fragments in the circulation (circulating free DNA [cfDNA]) that are of tumor origin, is a clinically available and emerging genetic biomarker.[11] It has shown to be able to provide detailed insight into the molecular alterations and evolving progression of tumors under treatment.[4,5,11] In patients with NSCLC, numerous studies have shown that a decrease of mutant gene levels in ctDNA correlates to the therapeutic response of TKIs.[5] In another model-based study, the relative change of concentrations of driver mutation in ctDNA from the estimated baseline was shown to be predictive of disease progression of patients with NSCLC.[12] Further research on the correlation between ctDNA measurements and tumor size dynamics would be beneficial to understanding the evolutionary development of treatment resistance and the value of ctDNA.

In the current study, we aimed to develop a model to understand and characterize tumor dynamics and the development of drug resistance in patients with NSCLC treated with erlotinib. First, a population PK model of erlotinib was developed and thereafter applied to investigate the exposure-tumor inhibition relationship of erlotinib. Tumor dynamics' models accounting for tumor heterogeneity, with or without a pre-existing resistance component, and drug exposure-dependent treatment effects, were evaluated. Subsequently, we aimed to explore the correlation of the extent of somatic driver mutation in ctDNA at baseline with the tumor dynamics in patients with NSCLC.

METHODS

Patients and data

Intensively sampled PK data

Data obtained for the analysis included intensively sampled erlotinib concentration-time curves from 29 patients from two previous food interaction PK studies in patients with NSCLC who were treated with erlotinib for an activating EGFR mutation.[13,14] Erlotinib was administrated orally once daily with a dosage of 50–150 mg. PK samples were collected before drug intake and at 0.5, 1, 1.5, 2, 2.5, 3, 3.5, 4, 6, 8, 12, and 24 h after drug administration at steady-state. The studies were performed at the Erasmus MC Cancer Institute in Rotterdam, The Netherlands, and the details of the studies' design can be found in previous publications.[13,14] For the current study, only the data in the control arms that were sampled after receiving erlotinib with water and without concomitant esomeprazole were included, which aimed to be consistent with real-world patients. Details about the selected patient

population are presented in Table 1 (intensively sampled PK data [$N = 29$]).

Patients' demographic information, including age, sex, weight, height, and additional laboratory test results, including creatinine, estimated glomerular filtration rate, albumin, total bilirubin, aspartate aminotransferase, alanine aminotransferase, and alkaline phosphatase were collected for covariate analysis.

PK-PD data

In addition, longitudinal measured tumor sizes under standard clinical care conditions as well as sparsely sampled intended trough erlotinib concentrations were also collected from 18 patients with NSCLC who participated in the START-TKI study (NCT05221372), which is a prospective, observational multicenter, real-world data study.[6] Erlotinib was administrated orally once daily with a dosage of 75–150 mg. The tumor size measurements, that is, the sum of the longest diameters (SLDs; mm) of target lesions, were assessed by Response Evaluation Criteria in Solid Tumors (RECIST version 1.1).[15] Additional data on dosing information, ctDNA data on variant allele frequency (VAF) of mutant genes over time, and concentrations of cfDNA over time from these patients were also collected. The detailed methods of cfDNA isolation and next-generation sequencing process have earlier been described.[6] Patients' demographic information and laboratory test results, as mentioned above, were also collected for potential covariate analysis. Details about this population are presented in Table 1 (PK/PD data [$N = 18$]).

The studies from which the data were obtained were previously approved by the local ethics committee and were registered in the Dutch Trial Registry. Written informed consent was obtained from all patients prior to these studies, including the use of data for further studies. For the current study, the data were shared anonymously and all procedures were performed in accordance with relevant guidelines and the Declaration of Helsinki, so no additional informed consent had to be obtained.

Population PK model

Based on the collected PK data, a population PK model was developed to characterize the erlotinib PK profiles of included patients. The intensively sampled PK data and the sparsely sampled PK data from patients involved in the START-TKI study were combined for the model development.

One- and two-compartment models with first-order absorption, with or without lag time, and first-order

TABLE 1 Baseline patients' characteristics and the collected data.

| | Intensively sampled PK data | | PK/PD data | |
| | (N = 29) | | (N = 18) | |
	Median	Range	Median	Range
Age (years)	63	35–78	66	48–78
Sex (N)				
Male	13 (44.8%)		5 (27.8%)	
Female	16 (55.2%)		13 (72.2%)	
Weight (kg)	74	50–102	69.5	46.1–109
Height (cm)	173	152–202	169	154–180
Serum creatinine (μmol/L)	82	47–138	66	59–192
eGFR (mL/(min.1.73 m^2))	71	46–100	84.5	23–103
AST (IU/L)	29	13–40	21.5	14–37
ALT (IU/L)	25	10–83	18	6–43
Albumin (g/L)	41	32–48	42.5	34–51
ALP (U/L)	85	53–157	87.5	3–798
Bilirubin (μmol/L)	8	3–58	6.5	3–14
Erlotinib starting dose (N)				
150 mg	25 (86.2%)		18 (100%)	
100 mg	3 (10.3%)		0	
50 mg	1 (3.4%)		0	
N of concentrations per patient	13	13–13	8 (N = 2 no data)	1–20
N of SLD per patient	–	–	7	2–18
N of ctDNA/cfDNA data per patient	–	–	3	1–4

Abbreviations: ALP, alkaline phosphatase; ALT, alanine aminotransferase; AST, aspartate aminotransferase; cfDNA, circulating free DNA; ctDNA, circulating tumor DNA; eGFR, estimated glomerular filtration rate; PD, pharmacodynamic; PK, pharmacokinetic; SLD, sum of longest diameters.

elimination were explored as the structural model. A combined proportional and additive model was applied to characterize the residual error. Parameters were assumed to be log-normally distributed. A random variability on bioavailability (F) was also incorporated while the typical value of F was fixed to 1 to account for the interindividual variability (IIV) on F, which is shared by the apparent PK parameters (clearances and distribution volumes) making them correlated, and other sources of positive correlation between parameters.[16,17] This approach has been applied to stabilize the model and reduce the unexplained IIV in the apparent PK parameters.[18,19] The structural model was selected based on biological plausibility and the objective function value (OFV).

Patients' demographic information and laboratory test results were then investigated as covariates using the stepwise covariate modeling function of Perl-speaks NONMEM (version 4.9). The effect of all covariates on erlotinib clearance and that of weight, height, and albumin on the apparent distribution volume of the central compartment were investigated. The relationship between F and dose level was not explored because the majority of patients received the same dose level. Model selection was based on the reduction in OFV (a likelihood ratio test) assuming a χ^2 distribution, a reduction in IIV, and physiological plausibility. The p values were set as 0.05 and 0.01 for the forward selection and backward elimination process, respectively. A more detailed description of the covariates analysis can be found in Appendix S1.

The final model was evaluated with goodness-of-fit (GOF) plots, visual predictive checks (VPC) based on 1000 simulations, and bootstrap with 1000 resampled datasets. In addition, the percentage where the predicted area under the curve (AUC) falls within 80%–120% of the corresponding observed AUC (estimated with trapezoidal rules method) was calculated for the full concentration-time curves to evaluate the model. The percentage where the predicted trough concentrations fall within 80%–120% of the corresponding observations was also estimated for the data from the START-TKI study.
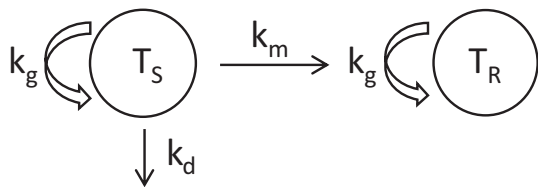
FIGURE 1 Graphical structure of the tumor dynamics model.

Tumor dynamics model

The dynamics of tumor sizes during erlotinib treatment, which was represented by SLD (mm) of target lesions, was characterized accounting for tumor heterogeneity. Tumor tissue was assumed to consist of a sensitive clonal population (T_S) and a resistant clonal population (T_R). Models considering (1) only acquired resistance and no primary resistance (i.e., baseline $T_R [T_{R\_0}] = 0$), and (2) both primary and acquired resistance (i.e., $T_{R\_0} \neq 0$ and was estimated), with or without a drug exposure-dependent decay, were explored. Considering the amount of available data, the baseline tumor sizes were fixed to the observed values to ensure the stability of the model. The model structure is shown in Figure 1 and Equations 1–4, where k_g represents the growth rates of T_S and T_R, k_m represents mutation rate, and k_d represents tumor decay rate due to treatment. For the models exploring the exposure-dependent treatment effect, the tumor decay rate was assumed to depend on erlotinib exposure and a simple linear relationship was assumed (Equation 2). A nonlinear relationship with a maximum effect (E_{max}) model was also explored. The erlotinib exposure was defined as the erlotinib concentration, effectively as the trough concentration at the tumor size monitoring timepoint, which was the exposure metric of interest for erlotinib exposure-response analysis and is relatively easy to measure in clinical practice. The time-varying erlotinib concentrations were simultaneously predicted with the individual PK parameters obtained from the PK model and incorporated into the tumor dynamics model. The IIV of parameters were evaluated and parameters were assumed to be log-normally distributed. The combined proportional and additive model was applied to characterize the residual error. The model fit was evaluated by OFV and Akaike information criterion (AIC). The best fitted model was evaluated with GOF plots and VPC considering the censoring of data due to progression defined by RECIST version 1.1.[15]

$$\frac{dT_S}{dt} = k_g \cdot T_S - k_d \cdot T_S - k_m \cdot T_S \qquad (1)$$

$$k_d = \begin{cases} k_d, \text{for the model without exposure} - \text{dependent decay} \\ k_d \cdot \text{Exposure, for the model with exposure} - \text{dependent decay} \end{cases}$$
$$(2)$$

$$\frac{dT_R}{dt} = k_m \cdot T_S + k_g \cdot T_R \qquad (3)$$

$$TS = T_S + T_R \qquad (4)$$

Genetic biomarkers and tumor dynamics

The correlation of baseline ctDNA measurements, including *EGFR* mutation levels and the presence of *TP53* mutations, with tumor dynamics' parameters (k_g, k_m, and k_d) were explored graphically. Patients were separated into groups based on (1) whether their baseline mutant *EGFR* VAF was less than or greater than or equal to the median value, or the measurements were unavailable, or (2) whether patients had a *TP53* mutation at baseline or not, or the results were unavailable. The correlation between baseline cfDNA concentrations and tumor dynamics' parameters was also explored by separating patients into groups based on the median value to investigate the informativeness of cfDNA compared to ctDNA.

Furthermore, the influence of baseline ctDNA measurements and cfDNA concentrations on k_g, k_m, and k_d were evaluated as categorical covariates in the tumor dynamics model. The *EGFR* mutation levels and the cfDNA concentrations were categorized based on the corresponding median values as described above. When a sample was missing, it was assigned to the third category and a sensitivity analysis was performed by evaluating models with and without the covariate for a dataset where the data from patients with missing covariates were removed. A significant correlation was defined as a decrease in OFV by more than 3.84 ($p < 0.05$, degree of freedom = 1, assuming $\chi 2$ distribution).

Software and estimation methods

The population modeling analysis in this study was performed with NONMEM (version 7.4.4, ICON Development Solutions). Parameters were estimated using the first order conditional estimation method with interaction. Data management and plot generation were performed with R statistics software (version 4.2.1; R Foundation for Statistical Computing).

RESULTS

Patients and data

The intensively sampled erlotinib concentration-time curves were obtained from 29 patients ($N = 377$, 13

TABLE 2 Parameter estimates of the population pharmacokinetics model.

Parameters	Explanation	Estimate (RSE%)	IIV (CV%) (RSE%) [shrinkage]	Bootstrap Median	Bootstrap 95% CI
CL/F (L/h)	Apparent clearance	4.10 (5%)	15.7% (31%) [48%]	4.09	3.68–4.47
Vc/F (L)	Apparent distribution volume of the central compartment	142 (7%)	20.3% (31%) [43%]	142	125–162
Vp/F (L)	Apparent distribution volume of the peripheral compartment	2420 (12%)	–	2462	1768–8043
Q/F (L/h)	Apparent distribution clearance	0.548 (40%)	194.4% (15%) [28%]	0.542	0.188–1.24
K_a (/h)	Absorption rate constant	1.61 (23%)	124.5% (15%) [18%]	1.68	1.03–2.65
T_{lag} (h)	Absorption lag time	0.400 (5%)	–	0.400	0.358–0.428
F	Bioavailability	1 fixed	16.3% (31%) [37%]	1 fixed	–
Residual errors					
Prop. err. (CV%)	Proportional residual error	15.4 (6%)	[10%][a]	15.3	–
Add. err. (SD, ng/mL)	Additive residual error	44.5 (25%)	[10%][a]	43.4	–

Abbreviations: CI, confidence interval; CV, coefficient of variation; IIV, interindividual variability; RSE, relative standard error; SD, standard deviation.

[a]Epsilon shrinkage.

samples per patient). The SLD measurements ($N = 155$) as well as additionally sampled erlotinib concentrations ($N = 146$), ctDNA measurements ($N = 50$), and cfDNA concentrations ($N = 50$) were collected from 18 real-world patients with NSCLC from the START-TKI study. For these 18 patients, the median time period when the SLD measurements were available is 264 days since the start of the treatment (range from 20 to 1168 days). All included patients had an event of disease progression ($n = 16$) or death ($n = 2$), and the use of erlotinib was stopped after the physician was sure that progression occurred. The data were censored after the stop of treatment.

The obtained erlotinib concentration data over time are presented in Figure S1. None of the collected data was below the lower limit of quantification. The median baseline tumor size (SLD) of the included patients was 76.6 mm (range: 29–116 mm). Out of the 146 obtained concentrations, 125 were measured at greater than or equal to 20 h after the last drug intake (trough concentrations) with a median of 842 ng/mL and range of 318–1834 ng/mL. Activating *EGFR* variants (including exon 19 deletions [$N = 11$] and *EGFR* p.L858R [$N = 6$] and p.K852R [$N = 1$] mutations) were detected in the tumor biopsies of all 18 patients.[6] The plasma cfDNA samples at the start of treatment were available from 12 out of 18 patients. The median baseline cfDNA concentration was 1.44 ng/μL (range from 0.77 to 3.65 ng/μL). The genetic variants that are of tumor origin (*EGFR* variants and *TP53* mutations) in cfDNA samples were also detected (i.e., ctDNA measurements). The primary *EGFR* variants were detected from baseline samples of eight out of 12 patients, which include exon 19 deletions ($N = 6$) and *EGFR* p.L858R ($N = 1$) and p.K852R ($N = 1$) mutations, and no primary *EGFR* variant was detected at baseline for the rest of the four patients. The median baseline *EGFR* VAF was 1.74% (range from 0% to 62.74%). The obtained VAF of primary *EGFR* variants over time are shown in Figure S2. Furthermore, a *TP53* mutation was detected in four patients at baseline and the *EGFR* p.T790M mutation was detected in three patients during erlotinib treatment. The baseline characteristics and the data contributed by each patient are summarized in Table 1.
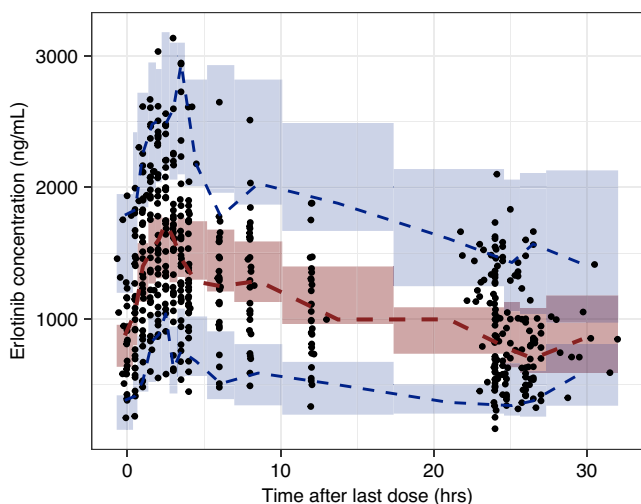
Population PK model

A two-compartment population PK model with first-order absorption with lag time and first-order elimination was developed and showed to best fit the obtained PK data. Compared to the one-compartment model, the OFV of the selected model decreased by 27.5 ($p < 0.01$, degree of freedom = 3), indicating an improvement in the model

fit. None of the tested covariates was identified to have significant effect on the PK parameters. The parameter estimates of the PK model are presented in Table 2. The relative standard errors (RSEs) were less than or equal to 25% for all parameters except for apparent distribution clearance (Q/F; 40%), indicating acceptable estimation precision. High estimates for IIV on Q/F and absorption rate constant (K_a) were observed (coefficient of variation [CV%] > 100%), with shrinkages less than 30%. The parameter estimates were also in good agreement with the bootstrap results (Table 2).

The GOF plots of the final PK model demonstrated a good concordance between the model predictions and observations (Figure S3). The conditional weighted residual errors (CWRES) were randomly distributed around zero without obvious trends over population predictions, but with a slight trend over time between 6 and 8 h after the last drug intake. The VPC plot (Figure 2) shows that the observed data can be adequately predicted by the developed model. Additionally, 100% of the model predicted AUC and 82.4% of the model predicted C_{trough} were within 80%–120% of their corresponding observations.

Tumor dynamics model

The tumor dynamics modeling results showed that the model accounting for acquired resistance only could adequately fit the data. The model that assumed the presence

FIGURE 2 VPC of the developed population PK model. The blue dashed lines represent 95th and 5th percentiles of the observations, the red dashed line represents the 50th percentile of the observations, the blue shaded areas represent 95% confidence interval of the 95th and 5th percentiles based on the simulations respectively, and the red shaded area represents 95% confidence interval of the 50th percentile based on the simulations. VPC, visual predictive check; PK, pharmacokinetic.

TABLE 3 Parameter estimates of the tumor dynamics models without or with baseline ctDNA data incorporated.

| Parameters	Description	Model without covariate		Model with baseline ctDNA data as a covariate	
		Estimate (RSE%)	IIV (CV%) (RSE%) [shrinkage%]	Estimate (RSE%)	IIV (CV%) (RSE%) [shrinkage%]
k_g (/day)	Tumor growth rate constant	0.000799 (13%)	60.3% (27%) [26%]	0.00204 (25%)	16.6% (152%) [57%]
f_1	k_g change fraction when mutant *EGFR* VAF <1.74%	–	–	0.334 (28%)	–
f_2	k_g change fraction when baseline ctDNA data was unavailable	–	–	0.281 (28%)	–
k_d (/day)	Tumor decay rate constant	0.0121 (19%)	68.4% (26%) [8%]	0.0123 (18%)	66.2% (22%) [7%]
k_m (/day)	Mutation rate constant	0.00911 (2%)	56.5% (25%) [19%]	0.00824 (18%)	57.9% (32%) [15%]
T_{S_0} (mm)	Baseline size of sensitive clonal population	Observed baseline	–	Observed baseline	–
T_{R_0} (mm)	Baseline size of resistant clonal population	0 fixed	–	0 fixed	–
Residual errors					
Prop. err. (CV%)	Proportional residual error	7.54% (13%)	[12%][a]	7.67% (14%)	[12%][a]
Add. err. (SD, mm)	Additive residual error	1.17 (38%)	[12%][a]	1.13 (9%)	[12%][a]

Abbreviations: ctDNA, circulating tumor DNA; CV, coefficient of variation; IIV, interindividual variability; RSE, relative standard error; SD, standard deviation; VAF, variant allele frequency.

[a]Epsilon shrinkage.

of primary resistance did not show an improved fit to the available data ($p > 0.05$, OFV decreased by 0.731 and AIC increased by 1.269, degree of freedom = 1). The typical estimate of T_{R_0} in this model was 4.51 mm which accounted for a small proportion (5.9%) of the median baseline tumor size (Table S1). Therefore, the pre-exiting resistance component was ultimately not included in the model. Furthermore, the OFV and AIC of the model incorporating an exposure-dependent decay increased by 1.441 compared with the base model, indicating no improvement in the model fit. Therefore, the exposure-dependent drug effect was not included in the final model.

The parameter estimates of the final tumor dynamics model are shown in Table 3 (model code in Appendix S2). The RSEs of the parameter estimates were all less than 30%, indicating acceptable estimation precision. High estimates for IIV of the estimated tumor dynamics parameters were observed (CV% > 60%). The GOF plots demonstrated a sufficient fit of the developed model to the data (Figure S4). The VPC considering the censoring of data due to progression showed that the model-predicted intervals adequately captured the distribution of observations (Figure 3).

Genetic biomarkers and tumor dynamics

The baseline results regarding ctDNA measurements and cfDNA concentrations were available from 12 out of 18
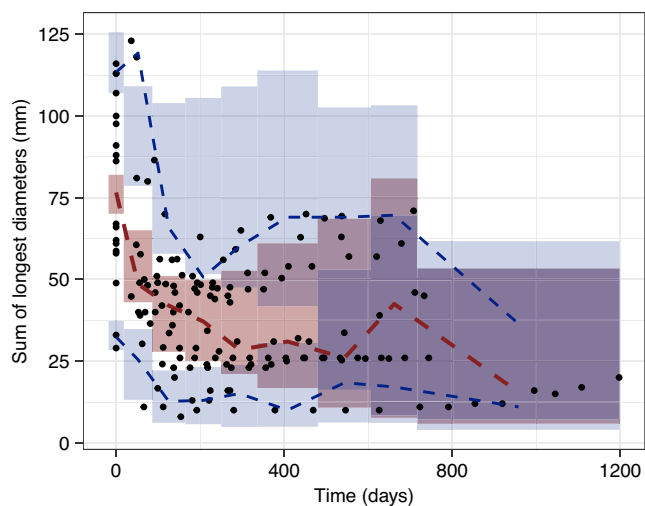
FIGURE 3 VPC considering dropout of the developed tumor dynamics model. The blue dashed lines represent 95th and 5th percentiles of the observations, the red dashed line represents the 50th percentile of the observations, the blue shaded areas represent 95% confidence interval of the 95th and 5th percentiles based on the simulations respectively, and the red shaded area represents 95% confidence interval of the 50th percentile based on the simulations. VPC, visual predictive check.

patients and missing for six patients. No correlation was observed between baseline mutant *EGFR* VAF and cfDNA concentrations. According to the exploratory plots, patients with baseline mutant *EGFR* VAF greater than or equal to 1.74% had relatively high k_g and k_m estimates, and slightly higher k_d estimates than patients with mutant *EGFR* VAF less than or equal to 1.74% (Figure 4). In addition, for patients with a *TP53* mutation at baseline, the k_g and k_m estimates were relatively high compared to patients without *TP53* mutations, and comparable k_d estimates were observed (Figure 4). The association between baseline cfDNA concentrations and tumor dynamics' parameters is shown in Figure S5. Patients with baseline cfDNA concentration greater than or equal to 1.44 ng/μL showed to have higher k_g and lower k_d estimates than patients with baseline cfDNA concentration less than or equal to 1.44 ng/μL, and comparable k_m estimates were observed.

When exploring the covariate effect of the baseline genetic biomarkers in the tumor dynamics model, the correlation between baseline mutant *EGFR* VAF and k_g was identified to be most significant when assigning the missing values as a separate category (OFV decreased by 11.6, $p < 0.01$, degree of freedom = 2). This correlation remained to be significant when removing the data of patients with missing covariate from the dataset (OFV decreased by 4.6, $p < 0.05$, degree of freedom = 1). The differences in k_m or k_d among patients' groups with different baseline mutant *EGFR* VAF levels were shown to be not significant. Additionally, the correlations between the presence of a *TP53* mutation and tumor dynamics parameters were also not significant in the covariate analysis. The parameter estimates of the model with baseline mutant *EGFR* VAF as the covariate are shown in Table 3. The typical k_g estimate in patients with baseline *EGFR* VAF greater than or equal to 1.74% was 0.00204 day^{-1}, which is higher than the estimate for the whole population (0.000799 day^{-1}). The typical k_g estimate in patients with baseline *EGFR* VAF less than or equal to 1.74% was 33.4% of that in patients with baseline *EGFR* VAF greater than or equal to 1.74%, whereas the difference between patients with baseline *EGFR* VAF less than or equal to 1.74% and with unknown mutant *EGFR* level was not significant. The inclusion of mutant *EGFR* VAF in the model decreased the CV% of k_g from 60.3% to 16.6%, whereas the corresponding RSE increased. The population predictions of the model also improved according to the GOF plots (Figure S6).

DISCUSSION

In this study, the tumor dynamics and the development of drug resistance in patients with NSCLC undergoing
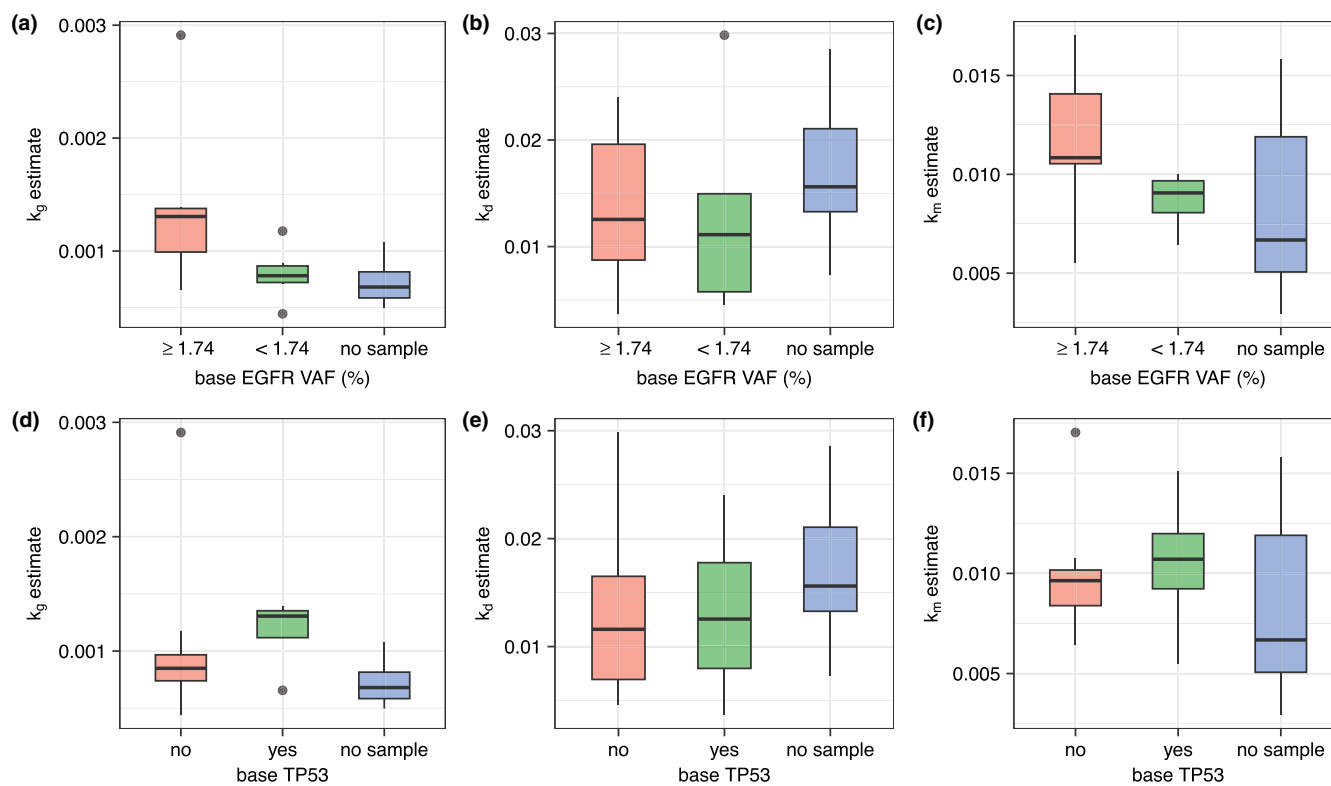
FIGURE 4 Parameter estimates from the tumor dynamics model versus baseline plasma circulating tumor DNA (ctDNA) measurements on primary mutant *EGFR* variant allele frequency and *TP53* mutation. VAF, variant allele frequency.

erlotinib treatment was characterized with a mathematical model accounting for tumor heterogeneity. Incorporating the erlotinib exposure into the model was also explored. The potential correlation between baseline genetic biomarkers and parameters that characterize tumor dynamics was identified with exploratory plots and confirmed with the model.

To facilitate the investigation on the exposure-tumor inhibition relationship, a population PK model of erlotinib was first developed. The estimated clearance is comparable to what has been reported previously (4.10 L/h vs. 3.64–4.71 L/h).[20–23] Due to a lack of data, previously reported covariates on erlotinib PK, including the smoking status, co-medications, and alpha-1-acid glycoprotein, could not be investigated in our analysis.[20,23] The CV% of K_a and Q/F was estimated to exceed 100%. For K_a, this high IIV estimate might be because it covers the variability in the lag time of absorption. Considering the amount of available data, these IIV estimates may not be precise. However, this does not affect the predictive ability of the PK model for the intended use in this study. The performance of the model was confirmed by the model evaluation results. However, a trend in CWRES over time between 6 and 8 h after the last drug intake was observed. This is considered to be due to the double peaks that were observed in the obtained data: data from 18 out of 29 patients who provided intensively sampled PK data demonstrate increased drug

concentrations at 6–8 h. The possible explanation could be the delayed disintegration of the tablets, food intake,[24,25] or possible enterohepatic circulation, although the latter has not been reported in literature before. These observed double peaks could not be captured by the current PK model, nor by a model considering dual first-order absorption with different lag times. Nevertheless, the model showed to be able to adequately predict the AUC of individual concentration-time curves as well as the trough concentrations which are of interest to be linked to the tumor dynamics. Therefore, the developed PK model was considered to be valid to support our study.

For the tumor size dynamics, a model accounting for intra-tumor heterogeneity and acquired resistance was shown to adequately fit the obtained data, and considering primary resistance was not favored based on the available data. This may indicate that for patients with NSCLC with an activating *EGFR* mutation, it is mainly the acquired resistance, which may be due to the acquisition of *EGFR* p.T790M mutation or other mechanisms, that limits the treatment response. Among previously reported model-based studies on tumor size dynamics in patients with NSCLC undergoing erlotinib treatment, one study also considered tumor heterogeneity.[26] Their results also showed that the models with and without primary resistance could describe the data equally well, even though erlotinib was used as a second-line treatment in their study.[26] However,

it is worth noting that the model presented in the current study is empirical and simplifies the complex process of the emergence of treatment resistance. Previously, several mechanistic models have been proposed to provide quantitative insight into this process.[27,28] The relatively limited amount of data in the current analysis prohibits the implementation of more mechanistic models and therefore may limit the mechanistic interpretation. In fact, the presence of *TP53* mutations may indicate the presence of primary resistance.[29,30] However, *TP53* mutations were only detected in four out of 18 patients which may be unable to provide significant impact to our model. Nonetheless, this more empirical approach does take into account the existence and interaction among multiple clonal populations which are crucial for understanding resistance development.[28] We do consider this approach relevant for exploring optimal guided drug treatment in real-world clinical oncology practice where extensive data are normally sparse. Furthermore, the current approach can serve as a basis for building more mechanistic-based models when more extensive data are available.[28] The growth rates of treatment-sensitive and resistant clonal populations were assumed to be the same in the model. This was because of the lack of identifiability of separate growth rates due to the limited amount of data.

The current study did not identify a clear exposure-tumor inhibition relationship within the current concentration range (the median predicted drug concentrations at the tumor size monitoring time points was 992 ng/mL [range of 284–1554 ng/mL]), neither when assuming a nonlinear relationship with the E_{max} model. A dose-tumor inhibition relationship was also explored but no clear relationship was identified. This might be because the treatment effect has already been saturated. The dose level selected for erlotinib (i.e., 150 mg daily) is the maximum tolerated dose, under which the average C_{trough} at steady-state is well above what is required for the required erlotinib activity and considered to be sufficient to provide a high anti-neoplastic effect.[31] This lack of relationship is in line with previous clinical studies where no significant correlation between erlotinib exposure and response has been identified.[32–34] One study also showed that increased erlotinib exposure had less impact on the antitumor effects in *EGFR* mutation-positive patients.[35] As an exposure-response relationship was not identified, we could not investigate the influence of drug exposure on the evolving tumor progression in this case. However, this result suggests that there is a potential option to decrease the dose of erlotinib to target for a lower concentration range that still ensures sufficient efficacy but can be better tolerated, especially because a significant proportion of erlotinib-treated patients can have severe toxicity.[6] The US Food and Drug Administration

has recently proposed the Project Optimus which also encourages to improve dose selection and optimization for oncology drugs by accounting for both efficacy and tolerability rather than automatically selecting the maximum tolerated dose.[36,37] A recent study has already suggested an optimized starting dose of 50–60 mg/day for erlotinib and a concentration range of 150–310 ng/mL for personalized erlotinib treatment in patients with NSCLC considering both efficacy and tolerability.[38]

The correlation between baseline genetic biomarkers and parameters in tumor dynamics' model was investigated in this study. The VAF's of mutant *EGFR* and the presence of *TP53* mutations in ctDNA at baseline showed to have potential correlation with the estimated parameters in the tumor dynamics model (mainly k_g and k_m), especially that higher baseline *EGFR* VAF was significantly correlated with increased growth rate constant k_g. This indicates that patients with higher *EGFR* VAF at baseline may have a worse response to the treatment, which is in line with the clinical findings from a *EGFR* cohort in the START-TKI study (i.e., patients without detectable ctDNA at baseline had a lower rate of radiological progression).[6] An explanation could be the association between ctDNA levels and tumor burden.[11,39] Our result is also in line with previous findings that baseline concomitant *TP53* mutations may relate to worse clinical outcome in patients with NSCLC.[6] After incorporating baseline ctDNA measurements, the developed tumor dynamics model could better predict the tumor size dynamics in response to erlotinib treatment in patients with NSCLC in the population level (Figure S7), and the IIV of k_g was reduced from 60.3% to 16.6% (CV%). This finding also demonstrates the potential to use baseline ctDNA as an early biomarker to support decision making for the treatment of patients with NSCLC.[40] Nonetheless, it is worth noting that the inclusion of the covariate resulted in a relatively poor estimation of IIV on k_g (RSE increased to 152%), which is likely due to the small number of subjects in each category. Therefore, more data are desired for a more robust model and to validate the results.

This study also has some limitations. The results found in the current study are based on limited data from a limited number of patients, especially for genetic biomarkers. The unavailability of baseline cfDNA samples in six out of 18 patients could also impact the interpretation of the results, as well as the determination of the threshold value of *EGFR* VAF which was associated with increased growth rates. However, this study is one of the first that investigated the relationships among PK, tumor dynamics, and ctDNA measurements. Furthermore, because the data on detectable mutation levels in ctDNA are limited, the development of a model

for describing longitudinal ctDNA data was not feasible and only the baseline ctDNA measurements were included in the analysis, which, however, explored the value of ctDNA as an early biomarker. Additionally, the mutant *EGFR* VAF was only investigated as a categorical covariate, whereas the data range from 0% to 62.74% and correspond to multiple variants. Therefore, further analysis with more extensive data is warranted to validate the current results and to explore the correlation between the longitudinal ctDNA measurements and tumor size dynamics with models.

In conclusion, our study demonstrated that the model accounting for intra-tumor heterogeneity and acquired resistance can well-characterize the tumor size dynamics in patients with NSCLC during erlotinib treatment. No clear exposure-tumor inhibition relationship was identified within the current concentration range. A correlation between baseline ctDNA measurements and tumor growth rates was, however, identified which suggests that quantitative ctDNA measurements at baseline have the potential to be predictive of anticancer treatment response, and further study on more extensive longitudinal data is warranted. The developed model can potentially be further applied to design optimal treatment regimens that better overcome resistance.

AUTHOR CONTRIBUTIONS

A.Y., G.D.M.V., J.G.C.v.H., C.M.J.S., H.J.D., H.-J.G., L.E.F., A.-M.C.D., R.H.J.M., and D.J.A.R.M. wrote the manuscript.; D.J.A.R.M. and H.-J.G. designed the research. A.Y., G.D.M.V., J.G.C.v.H., C.M.J.S., H.J.D., H.-J.G., L.E.F., A.-M.C.D., R.H.J.M., and D.J.A.R.M. performed the research. A.Y., J.G.C.v.H., L.E.F., and D.J.A.R.M. analyzed the data.

FUNDING INFORMATION

CONFLICT OF INTEREST STATEMENT

The authors declared no competing interests for this work.

DATA AVAILABILITY STATEMENT

The datasets generated during and/or analyzed during the current study are available from the corresponding author on reasonable request.

ORCID

Anyue Yin https://orcid.org/0000-0001-9924-6040
Johan G. C. van Hasselt https://orcid.org/0000-0002-1664-7314
Christi M. J. Steendam https://orcid.org/0000-0002-8487-9344

Hendrikus Jan Dubbink https://orcid.org/0000-0002-2160-5207
Henk-Jan Guchelaar https://orcid.org/0000-0002-7085-1383
Lena E. Friberg https://orcid.org/0000-0002-2979-679X
Anne-Marie C. Dingemans https://orcid.org/0000-0001-6105-182X
Ron H. J. Mathijssen https://orcid.org/0000-0001-5667-5697
Dirk Jan A. R. Moes https://orcid.org/0000-0003-3219-253X

REFERENCES

1. Zhao B, Hemann MT, Lauffenburger DA. Modeling tumor clonal evolution for drug combinations design. *Trends Cancer*. 2016;2:144-158.
2. Sun X, Hu B. Mathematical modeling and computational prediction of cancer drug resistance. *Brief Bioinform*. 2018;19:1382-1399.
3. Nagano T, Tachihara M, Nishimura Y. Mechanism of resistance to epidermal growth factor receptor-tyrosine kinase inhibitors and a potential treatment strategy. *Cell*. 2018;7:212.
4. Oliveira KCS, Ramos IB, Silva JMC, et al. Current perspectives on circulating tumor DNA, precision medicine, and personalized clinical management of cancer. *Mol Cancer Res*. 2020;18:517-528.
5. Herbreteau G, Vallee A, Charpentier S, et al. Circulating free tumor DNA in non-small cell lung cancer (NSCLC): clinical application and future perspectives. *J Thorac Dis*. 2019;11:S113-S126.
6. Steendam CMJ, Veerman GDM, Pruis MA, et al. Plasma predictive features in treating EGFR-mutated non-small cell lung cancer. *Cancers (Basel)*. 2020;12:3179.
7. Barbolosi D, Ciccolini J, Lacarelle B, Barlesi F, Andre N. Computational oncology — mathematical modelling of drug regimens for precision medicine. *Nat Rev Clin Oncol*. 2016;13:242-254.
8. Buil-Bruna N, Lopez-Picazo JM, Martin-Algarra S, Troconiz IF. Bringing model-based prediction to oncology clinical practice: a review of pharmacometrics principles and applications. *Oncologist*. 2016;21:220-232.
9. Kimko H, Pinheiro J. Model-based clinical drug development in the past, present and future: a commentary. *Br J Clin Pharmacol*. 2015;79:108-116.
10. Yin A, van Hasselt JGC, Guchelaar HJ, Friberg LE, Moes D. Anti-cancer treatment schedule optimization based on tumor dynamics modelling incorporating evolving resistance. *Sci Rep*. 2022;12:4206.
11. Wan JCM, Massie C, Garcia-Corbacho J, et al. Liquid biopsies come of age: towards implementation of circulating tumour DNA. *Nat Rev Cancer*. 2017;17:223-238.
12. Janssen JM, Verheijen RB, van Duijl TT, et al. Longitudinal nonlinear mixed effects modeling of EGFR mutations in ctDNA as predictor of disease progression in treatment of EGFR-mutant non-small cell lung cancer. *Clin Transl Sci*. 2022;15:1916-1925.
13. van Leeuwen RW, Peric R, Hussaarts KG, et al. Influence of the acidic beverage cola on the absorption of erlotinib in patients with non-small-cell lung cancer. *J Clin Oncol*. 2016;34:1309-1314.

14. Veerman GDM, Hussaarts K, Peric R, et al. Influence of cow's milk and esomeprazole on the absorption of erlotinib: a randomized, crossover pharmacokinetic study in lung cancer patients. *Clin Pharmacokinet*. 2021;60:69-77.

15. Eisenhauer EA, Therasse P, Bogaerts J, et al. New response evaluation criteria in solid tumours: revised RECIST guideline (version 1.1). *Eur J Cancer*. 2009;45:228-247.

16. Mould DR, Upton RN. Basic concepts in population modeling, simulation, and model-based drug development – part 2: introduction to pharmacokinetic modeling methods. *CPT Pharmacometrics Syst Pharmacol*. 2013;2:e38.

17. Karlsson MO, Radojka S. Overview of oral absorption models and modelling issues. PAGE meeting website. Accessed November 25, 2023. Available from: https://www.page-meeting.org/default.asp?abstract=1044

18. Hennig S, Wainwright CE, Bell SC, Miller H, Friberg LE, Charles BG. Population pharmacokinetics of itraconazole and its active metabolite hydroxy-itraconazole in paediatric cystic fibrosis and bone marrow transplant patients. *Clin Pharmacokinet*. 2006;45:1099-1114.

19. Kamel B, Abuhelwa AY, Foster D, et al. Population pharmacokinetic modelling of febuxostat in healthy subjects and people with gout. *Br J Clin Pharmacol*. 2022;88:5359-5368.

20. Emoto-Yamamoto Y, Iida S, Kawanishi T, Fukuoka M. Population pharmacokinetics of erlotinib in Japanese patients with advanced non-small cell lung cancer. *J Clin Pharm Ther*. 2015;40:232-239.

21. Parra-Guillen ZP, Berger PB, Haschke M, et al. Role of cytochrome P450 3A4 and 1A2 phenotyping in patients with advanced non-small-cell lung cancer receiving Erlotinib treatment. *Basic Clin Pharmacol Toxicol*. 2017;121:309-315.

22. Endo-Tsukude C, Sasaki JI, Saeki S, et al. Population pharmacokinetics and adverse events of erlotinib in Japanese patients with non-small-cell lung cancer: impact of genetic polymorphisms in metabolizing enzymes and transporters. *Biol Pharm Bull*. 2018;41:47-56.

23. Evelina C, Guidi M, Khoudour N, et al. Population pharmacokinetics of erlotinib in patients with non-small cell lung cancer: its application for individualized dosing regimens in older patients. *Clin Ther*. 2020;42:1302-1316.

24. Rampaka R, Ommi K, Chella N. Role of solid lipid nanoparticles as drug delivery vehicles on the pharmacokinetic variability of erlotinib HCl. *J Drug Deliv Sci Technol*. 2021;66:102886.

25. Veerman GDM, Hussaarts K, Jansman FGA, et al. Clinical implications of food-drug interactions with small-molecule kinase inhibitors. *Lancet Oncol*. 2020;21:e265-e279.

26. Mistry HB, Helmlinger G, Al-Huniti N, Vishwanathan K, Yates J. Resistance models to EGFR inhibition and chemotherapy in non-small cell lung cancer via analysis of tumour size dynamics. *Cancer Chemother Pharmacol*. 2019;84:51-60.

27. Foo J, Michor F. Evolution of acquired resistance to anti-cancer therapy. *J Theor Biol*. 2014;355:10-20.

28. Terranova N, Girard P, Klinkhardt U, Munafo A. Resistance development: a major piece in the jigsaw puzzle of tumor size modeling. *CPT Pharmacometrics Syst Pharmacol*. 2015;4:320-323.

29. Canale M, Petracci E, Delmonte A, et al. Impact of TP53 mutations on outcome in EGFR-mutated patients treated with first-line tyrosine kinase inhibitors. *Clin Cancer Res*. 2017;23:2195-2202.

30. Ulivi P, Delmonte A, Chiadini E, et al. Gene mutation analysis in EGFR wild type NSCLC responsive to erlotinib: are there features to guide patient selection? *Int J Mol Sci*. 2014;16:747-757.

31. US Food and Drug Administration. Drug approval package: Tarceva (Erlotinib) Tablets (Application No.: 021743). Accessed September 14, 2023. https://www.accessdata.fda.gov/drugsatfda_docs/nda/2004/21-743_Tarceva.cfm

32. Yu H, Steeghs N, Nijenhuis CM, Schellens JHM, Beijnen JH, Huitema ADR. Practical guidelines for therapeutic drug monitoring of anticancer tyrosine kinase inhibitors: focus on the pharmacokinetic targets. *Clin Pharmacokinet*. 2014;53:305-325.

33. Verheijen RB, Yu H, Schellens JHM, Beijnen JH, Steeghs N, Huitema ADR. Practical recommendations for therapeutic drug monitoring of kinase inhibitors in oncology. *Clin Pharmacol Ther*. 2017;102:765-776.

34. Kenmotsu H, Imamura CK, Kawamura T, et al. Prospective evaluation of the relationship between response and exposure of total and unbound erlotinib in non-small cell lung cancer patients. *Cancer Chemother Pharmacol*. 2022;90:115-123.

35. Fukudo M, Ikemi Y, Togashi Y, et al. Population pharmacokinetics/pharmacodynamics of erlotinib and pharmacogenomic analysis of plasma and cerebrospinal fluid drug concentrations in Japanese patients with non-small cell lung cancer. *Clin Pharmacokinet*. 2013;52:593-609.

36. Fourie Zirkelbach J, Shah M, Vallejo J, et al. Improving dose-optimization processes used in oncology drug development to minimize toxicity and maximize benefit to patients. *J Clin Oncol*. 2022;40:3489-3500.

37. Shah M, Rahman A, Theoret MR, Pazdur R. The drug-dosing conundrum in oncology – when less is more. *N Engl J Med*. 2021;385:1445-1447.

38. Takeda Y, Ishizuka N, Sano K, et al. Phase I/II study of erlotinib to determine the optimal dose in patients with non-small cell lung cancer harboring only EGFR mutations. *Clin Transl Sci*. 2020;13:1150-1160.

39. Sanz-Garcia E, Zhao E, Bratman SV, Siu LL. Monitoring and adapting cancer treatment using circulating tumor DNA kinetics: current research, opportunities, and challenges. *Sci Adv*. 2022;8:eabi8618.

40. Bruno R, Chanu P, Kagedal M, et al. Support to early clinical decisions in drug development and personalised medicine with checkpoint inhibitors using dynamic biomarker-overall survival models. *Br J Cancer*. 2023;129:1383-1388. doi:10.1038/s41416-023-02190-5

SUPPORTING INFORMATION

Additional supporting information can be found online in the Supporting Information section at the end of this article.